

# Deterioration of Polypropylene/Silicon Dioxide Nanocomposites Before Oxidative Degradation

Jifang Li, Rui Yang, Jian Yu, Ying Liu

*Institute of Polymer Science and Engineering, Department of Chemical Engineering, Tsinghua University, Beijing 100084, People's Republic of China*

Received 17 November 2008; accepted 29 January 2009

DOI 10.1002/app.30126

Published online 19 March 2009 in Wiley InterScience (www.interscience.wiley.com).

**ABSTRACT:** The thermal aging of polypropylene (PP)/SiO<sub>2</sub> nanocomposite films was carried out at 130°C. In contrast to the widely accepted thermal oxidation mechanism, the film ruptured far before the carbonyl group was detected and without a noticeable reduction in the molecular weight. Observations with a polarizing optical microscopy and a scanning electron microscopy demonstrated that, instead of oxidative degradation, at least three other factors were responsible for the rapid deterioration of the PP/SiO<sub>2</sub> nanocomposites: (1) recrystallization during the thermal aging, which gave rise to a major volume contraction and, thus, great stress along the spherulite boundaries, which might have induced cracks there (another effect of

the recrystallization was the rejection of nanoparticles and defects to the spherulite boundaries, which, therefore, weakened the boundaries); (2) poor interfacial interaction between the matrix and the nanoparticles; and (3) large temperature changes, which created interfacial debonding because of the significant difference in the thermal expansion coefficients of PP and the nanoparticles. The results of this study extend the understanding of the thermal oxidative degradation mechanism of polymer materials. © 2009 Wiley Periodicals, Inc. *J Appl Polym Sci* 113: 601–606, 2009

**Key words:** degradation; nanocomposites; poly(propylene) (PP)

## INTRODUCTION

Recently, polymer nanocomposites and, in particular, polymer/layered silicate nanocomposites have attracted a great deal of attention because of the significant improvements they offer in terms of mechanical properties and gas barrier and fire-retardancy properties at very low filler concentrations and low densities.<sup>1–5</sup> They are even regarded as promising alternatives to steel in the automobile industry.<sup>6</sup>

In addition to mechanical properties, stability is another key factor in all applications. Many studies on the thermal and thermal oxidation stability of polymer nanocomposites have reported improved thermal stability with the addition of nanofillers. Blumstein<sup>7</sup> first pointed out that the increased thermal stability of poly(methyl methacrylate) nanocomposites was due to steric factors. The movements of poly(methyl methacrylate) chains intercalated between the clay lamellae were restricted, and greater thermal resistance was achieved. Gilman and coworkers<sup>8,9</sup> and Bertini et al.<sup>10</sup> proposed that the

barrier effect of clay char on the surface of the nanocomposite would contribute to the mass-transfer and heat-transfer barriers and, therefore, lead to a higher thermal stability in the polymer. Zanetti et al.<sup>11</sup> studied the thermal degradation of polypropylene (PP)/clay by thermogravimetric analysis (TGA). They suggested that clay played a catalytic role and favored the oxidative dehydrogenation–crosslinking–charring process and that it helped the surface polymer molecules to produce stable charred material, which provided a new shield layer to protect the matrix. The presence of clay also modifies the degradation mechanism of polyethylene and PP.<sup>11,12</sup> Qin et al.<sup>13</sup> proposed that, with the help of montmorillonite, the surface charred layer of PP that is formed would protect the interior from degradation and, thus, increase the thermal stability of polymer nanocomposites. The thermal oxidative degradation kinetics of PP/montmorillonite nanocomposites were studied by Lomakin et al.<sup>14</sup> Zhu et al.<sup>15</sup> and Xu et al.<sup>16</sup> argued that iron in the clay could act as a radical scavenger. Chen and Vyazovkin<sup>17</sup> studied the thermal and thermal oxidative degradations of polystyrene (PS)/clay nanocomposites prepared by *in situ* polymerization, using thermogravimetry–Fourier transform infrared spectroscopy and gas chromatography–mass spectrometry (GC–MS). They found a brushlike morphology of PS chains on the clay layers. This physical structure had a barrier effect on

Correspondence to: R. Yang (yangr@mail.tsinghua.edu.cn).

Contract grant sponsor: National Natural Science Foundation of China; contract grant number: 50603010.

the diffusion of free radicals, oxygen, and degradation products and stabilized the nanocomposite. TGA of carbon-nanofiber-filled PP showed that carbon nanofibers improved the thermal oxidation stability and fire retardancy of the material.<sup>18</sup>

The evidence for most of these improvements came from TGA results. However, TGA evaluation often shows conflicting results under different measurement modes. In Peprnicek et al.'s<sup>19</sup> research on the thermal stability evaluation of PP/clay nanocomposites, nonisothermal TGA measurement gave conflicting stability sequences for three kinds of clay-filled PP and neat PP when compared by the temperature corresponding to 2% ( $T_{0.02}$ ), 5% ( $T_{0.05}$ ), and 10% ( $T_{0.10}$ ) weight loss. When evaluated by an isothermal process, the TGA measurements showed a progressive deterioration of the thermal stability of the nanocomposites. Furthermore, TGA measurement only provides the thermal degradation behavior in the melt state. The thermal stability evaluation of polymer nanocomposites in the solid state is more meaningful from a practical point of view. Filho et al.<sup>20</sup> studied the thermal stability of PP/bentonite nanocomposites at 110°C. The degradation of the composites was more intense than the unfilled polymer because of the presence of acidic sites on the clay surface that acted as catalysts to the oxidation of the polymer and/or because of the salt decomposition, which initiated the free-radical degradation of PP. The modified clay had higher stability in the solid state than the natural clay. This may have been connected to a higher dispersion of clay particles, which reduced oxygen diffusion through the sample.

Although there are many literature reports concerning the thermal stability of PP/clay nanocomposites, few have been found on PP filled with other commercial nanofillers. The aim of this study was to evaluate the effect of nano-SiO<sub>2</sub> on the thermal stability of PP in the solid state (at 130°C). Herein, SiO<sub>2</sub> was introduced to improve the rigidity of the PP films.

## EXPERIMENTAL

### Materials

Isotactic PP (F1002, melt flow index = 1.7 g/10 min), obtained from Yanshan Petrochemical Co., Ltd. (Beijing, China), was used as received. Nano-SiO<sub>2</sub>, about 40 nm in diameter, was supplied by Zhejiang Zhoushan Mingri Nano-Material Co. (Zhejiang, China).

### Preparation

We prepared the PP nanocomposite by mixing and coextruding PP with 3 wt % SiO<sub>2</sub> nanoparticles in a twin-screw extruder (TE-34, Jiangsu Keya Chemical

Equipment Co., Ltd., Jiangsu, China). The operating temperatures from the hopper to the die were maintained at 200, 220, 220, 220, 220, and 210°C. After they were cooled in water, the extrudates were pelletized. The pellets were then dried and hot-pressed at 210°C into films about 30 μm in thickness with a pressure of about 10 MPa.

The thermal oxidative degradation of the PP and PP/SiO<sub>2</sub> films was carried out in an oven at 130°C for up to 80 h. One film (named PP-S-I) was taken out after 16 h and 30 h for characterization. It broke into pieces after 40 h, whereas neat PP maintained its shape for up to 450 h. Another film (named PP-S-C) was continuously heated up to 80 h without interference.

### Instrumentation

The oxidation of the PP nanocomposite films was determined with a Fourier transform infrared spectrometer (Nicolet 560; Madison, WI). We obtained the spectra by averaging 32 scans at a resolution of 4 cm<sup>-1</sup> in the range 4000–400 cm<sup>-1</sup>.

A high-temperature gel permeation chromatograph (Waters Alliance GPCV2000; Milford, MA) was used for the determination of the PP nanocomposite molecular weight and its distribution. Samples were dissolved in 1,2,4-trichlorobenzene at 150°C to obtain a very dilute solution with a concentration of 0.1 wt %. The molecular weight was calculated by reference to a standard on the basis of the universal calibration curve of PS.

The volatile degraded products of the PP nanocomposite were analyzed by an electron ionization mass spectrometer coupled with a pyrolysis GC-MS instrument (Shimadzu GCMS-QP5050A equipped with a PYR-4A pyrolyzer, Japan). Samples were placed in a small Pt tube and dropped into the furnace, which was preset and maintained at 300°C. After 30 s, the tube was taken out. The volatile products from the samples were carried by a helium carrier gas (flow rate = 1.1 mL/min, split ratio = 30 : 1) through the fused silica capillary column (DB-5, length = 30 m, inside diameter = 0.25 mm) and separated. The oven temperature was held at 50°C for 1 min, then raised at a rate of 8°C/min to 280°C, and held for 40 min. Each component was identified by the mass spectrometry detector at 70 eV, and the interface temperature was 250°C.

The morphologies of the PP nanocomposite were observed with scanning electron microscopy (SEM; Hitachi S-450, Honshu, Japan), with the secondary electron image being obtained at an accelerating voltage of 15–20 kV. The samples were coated with gold before observation to minimize the charging problem.

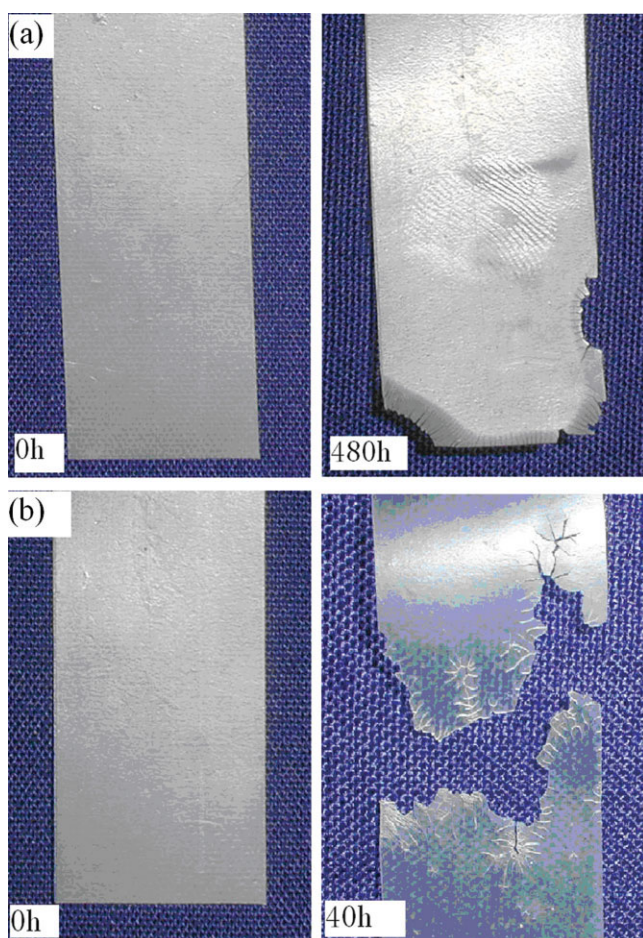


**Figure 1** Appearance of PP and PP-S-I before and after thermal treatment at 130°C: (a) neat PP and (b) PP-S-I. [Color figure can be viewed in the online issue, which is available at [www.interscience.wiley.com](http://www.interscience.wiley.com).]

To obtain polarizing micrographs, a Nikon light microscope with a digital camera was used to observe the spherulite morphologies.

## RESULTS AND DISCUSSION

The thermal oxidative degradation of a polymer is generally accepted to be a peroxidation chain reaction. Hydroperoxides thus formed may decompose to alkoxy radicals to initiate further oxidation, which leads to autoacceleration. In the solid-state degradation, the alkoxy radicals are more likely to undergo a  $\beta$ -scission reaction of the polymer chain, which produces carbonyl groups and alkyl radicals.<sup>21</sup> The consequent molecular weight decrease leads to the deterioration of the mechanical properties and can even damage the products.

However, embrittlement fracture during the thermal oxidative degradation of the PP/SiO<sub>2</sub> nanocomposites happened quite early, before any carbonyl group buildup was found by IR measurement. Figure 1 shows the appearance of PP-S-I and neat PP

before and after thermal treatment at 130°C, and the corresponding IR spectra are shown in Figure 2. For neat PP, no significant change in appearance happened after 480 h in the majority of the film, except for the spokewise cracks at the edges of the film, which were proved to be stress-induced cracks, which arose from the cutting procedure of the film. For PP-S-I, the film broke into pieces after only 40 h at 130°C.

For both neat PP and PP-S-I, no obvious oxidation happened when the films fractured. Although there might have been minor localized oxidized domains in the films, the carbonyl buildups were below the sensitivity threshold of the IR measurement. This phenomenon was interesting because it did not tally with the widely accepted thermal oxidation mechanism. To our knowledge, only Fayolle et al.<sup>22–24</sup> have ever reported embrittlement of PP before oxidation occurred. They attributed this to the molecular weight decrease of PP. However, in their experiments, the cracks did not appear in the stabilized PP film before 2700 h at 130°C, and nearly no chain scission was detected before 500 h. Therefore, other

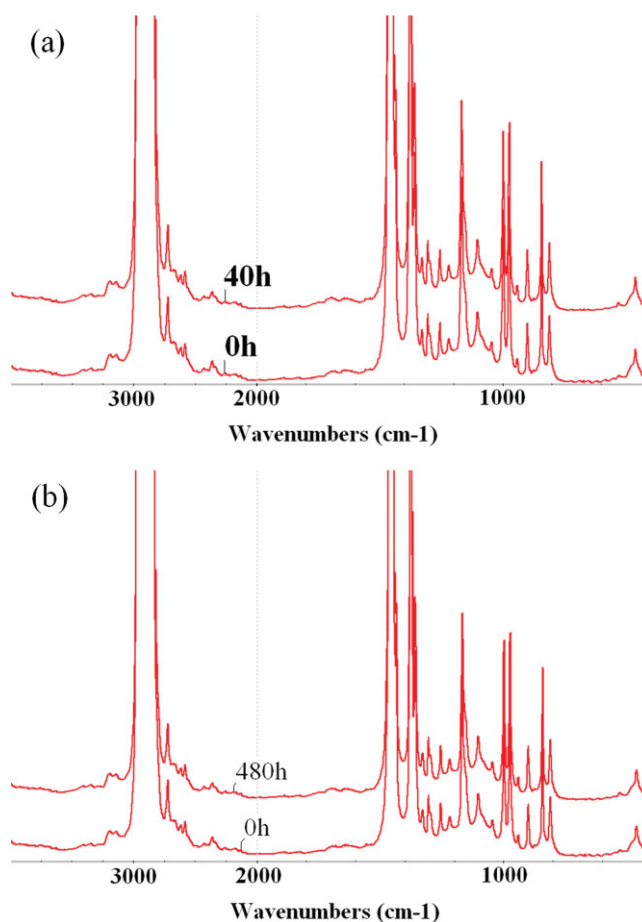


**Figure 2** IR spectra of PP and PP-S-I before and after thermal treatment at 130°C: (a) neat PP and (b) PP-S-I. [Color figure can be viewed in the online issue, which is available at [www.interscience.wiley.com](http://www.interscience.wiley.com).]

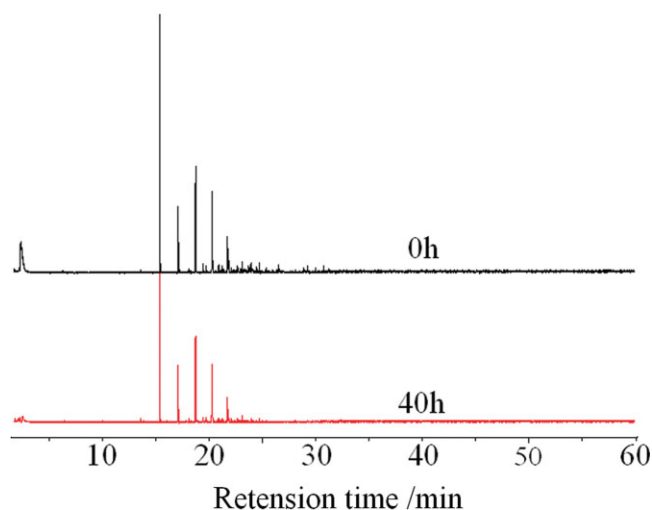


**Figure 3** Pyrograms of PP-S-I before and after thermal treatment. [Color figure can be viewed in the online issue, which is available at [www.interscience.wiley.com](http://www.interscience.wiley.com).]

factors must have been responsible for such a rapid fracture of the PP nanocomposite film. Because oxidation was negligible, the catalytic effect of nano-SiO<sub>2</sub> in the photooxidation reaction was not responsible for the fast damage of the films.

Fayolle et al.<sup>22,24</sup> reported a critical weight-average molecular weight of about 200 kg/mol for PP to undergo the ductile–brittle transition. The weight-average molecular weights of PP-S-I at 0 and 40 h were determined as 300,000 and 299,000, respectively. Therefore, there was no appreciable change in the molecular weight in such a short time. Also, the weight-average molecular weight was much higher than the critical value. So the rapid damage that occurred in PP-S-I may not have been due to chemical changes such as oxidation and molecular chain scissions.

The pyrolysis GC–MS analysis was carried out at 300°C to determine any volatile degradation product in PP-S-I after exposure. This temperature was chosen to evaporate the degraded small molecules and to prevent a large number of scissions of the main chain at the same time. Thus, the possible degraded products were highlighted without or with the least interference of fragments from the chain scissions at a high temperature.<sup>25</sup> Figure 3 shows the pyrograms of PP-S-I before and after the thermal treatment. Except for the same peaks that appeared in the 15–25-min range, which were attributed to alkanes with carbon numbers of 14–18, which came from stearate added in the polymerization process to neutralize the excess acidity of catalyst, there were no fragments coming from the chain scission in the sample after 40 h. This also demonstrated that there was no obvious oxidation or molecular scission in PP-S-I. Therefore, there may have been some physical fac-

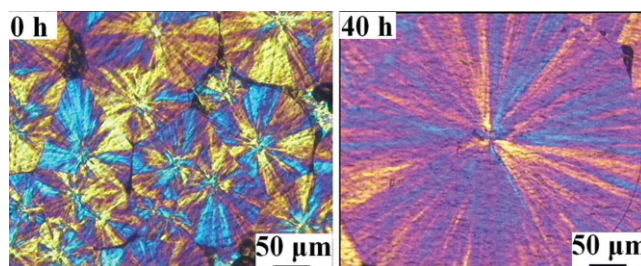


**Figure 4** Polarizing light micrographs of PP before and after 40 h of thermal treatment at 130°C. [Color figure can be viewed in the online issue, which is available at [www.interscience.wiley.com](http://www.interscience.wiley.com).]

tors rather than chemical structure changes that were responsible for the damage to the PP nanocomposite.

Recrystallization under high temperatures may have been responsible for the fracture. According to Calvert and Ryan,<sup>26</sup> during the crystallization process, impurities tend to be rejected from the growing spherulites. Consequently, there is an impurity-rich region at the spherulite boundary, and the boundary strength would be expected to decrease. These weak spherulite boundaries are often the place where fractures happen when the stress exceeds the critical value. The impurities in our study were not the oxidized species or low-molecular-weight components because there was no obvious oxidation or chain scission detected, but nano-SiO<sub>2</sub> particles, atactic PP molecules, and microvoids were detected instead. The stress should have resulted from the volume contraction, as a consequence of the recrystallization and/or temperature change. Figures 4 and 5 show photos of PP and PP-S-I, respectively, taken with a polarizing optical microscope before and after 40 h of exposure. It is clear that recrystallization happened during the thermal treatment at 130°C. At first, the diameters of the PP and PP-S-I spherulites were about 150 and 70 μm, respectively. There were a few amorphous domains along the spherulite edges (black region). After 40 h, the spherulite sizes of both PP and PP-S-I increased significantly, to

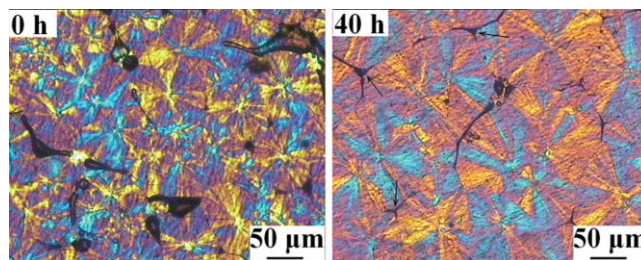


**Figure 5** Polarizing light micrographs of PP-S-I before and after 40 h of thermal treatment at 130°C. [Color figure can be viewed in the online issue, which is available at [www.interscience.wiley.com](http://www.interscience.wiley.com).]

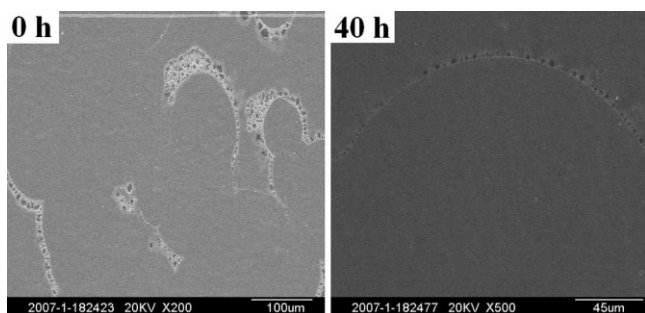


**Figure 6** SEM images of PP before and after 40 h of thermal treatment at 130°C.

about twice the original size, and the amorphous regions decreased significantly. Despite the significant recrystallization, there were no cracks in PP, whereas some cracks occurred in PP-S-I along the spherulite boundaries. The SEM observation demonstrated similar morphology changes (see Figs. 6 and 7, in which the early cracks in PP-S-I are more evident). This showed that the volume contraction resulting from the recrystallization should not have been the only reason for crack formation because there was no crack in PP with a higher crystallinity increment.<sup>27</sup> The cracks in PP-S-I may also have been related to the presence of nanoparticles, which gave rise to more minor spherulites and more spherulite boundaries. Consequently, boundary weakness became marked because the recrystallization process rejected nanoparticles to the spherulite boundaries. These weakened boundaries could not resist the stress coming from the volume contraction. Thus, cracks formed along the boundaries.

So, did the weakened boundaries dominate crack formation in the PP nanocomposite? To answer this question, we carried out another experiment. A PP nanocomposite film (PP-S-C) was heated at 130°C for 80 h without being removed intermittently. The morphology changes are shown in Figure 8. It was surprising that no cracks were found this time. This implied that the stress-induced cracks resulting from the violent temperature changes should have been

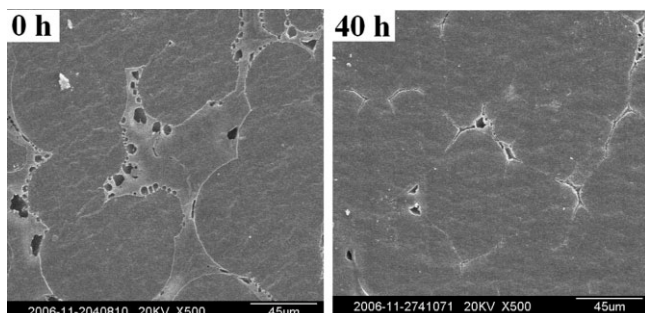


**Figure 7** SEM images of the PP/SiO<sub>2</sub> nanocomposites before and after 40 h of thermal treatment at 130°C.

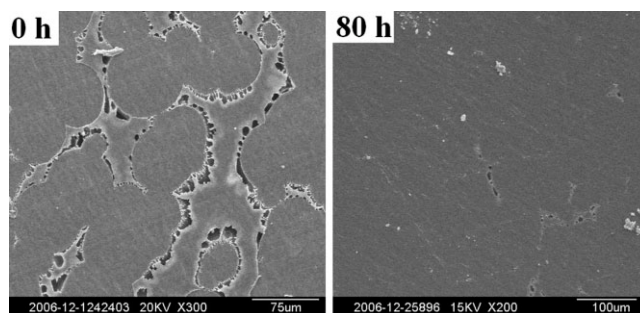


**Figure 8** SEM images of PP-S-C before and after 80 h of heating.

taken into account in the thermal oxidation fracture of the PP nanocomposite. As we know, a conventional aging test of a polymer material consists of intermittent removals from heating to monitor the physical and/or chemical changes that have taken place. During this process, samples undergo heating and cooling many times. Because of the difference in the expansion coefficient between nano-SiO<sub>2</sub> and the PP matrix, the shrinkage of the PP matrix was much more significant compared to that of the nano-SiO<sub>2</sub> particles and finally caused the interfacial debonding and voids (see Fig. 9). Poor cohesion between the matrix and the nanoparticles worsened the situation. When this was accompanied by the rejection of the nanoparticles to the spherulite boundaries, the interfacial debondings developed into cracks. As shown in Figure 8, aggregations of nanoparticles were also observed. This aggregation weakened the interfacial cohesion and made the debonding much easier. Therefore, it is reasonable that we found that the aged PP-S-C had no cracks. Although a significant recrystallization happened (most of the amorphous region and a large amount of bubbles and voids vanished), the spherulite boundaries and the interfacial cohesion were strong enough to resist the stress, even after a much longer test period (twice that of PP-S-I).

From the previous discussion, three factors, which were responsible for the early fracture of the PP/SiO<sub>2</sub> nanocomposite, can be described as follows:

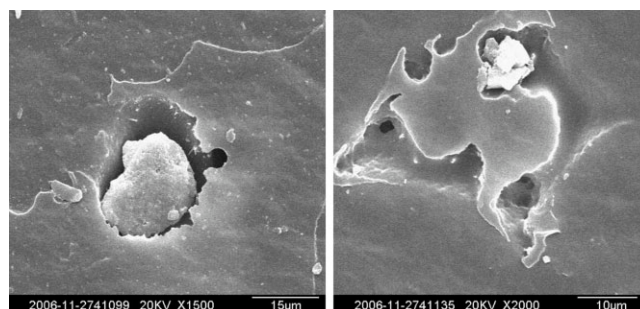


**Figure 9** Debonding of nanoparticles from the PP matrix.

1. Recrystallization, which caused great volume contraction and great stress on the spherulite boundaries.
2. Weak interfacial cohesion or weak spherulite boundaries, derived from the rejection of the nanoparticles and defects from the spherulites. The aggregation of nanoparticles worsened this situation.
3. Violent temperature changes, which may have caused the interfacial debonding of nanoparticles from the matrix.

For the PP film, although the recrystallization happened and it went through violent temperature changes, it remained unbroken because of the relatively strong spherulite boundaries with the absence of nanoparticles as impurities. For PP-S-C, the recrystallization and the weak interfaces/spherulite boundaries were not enough to make it rupture. In addition, the high activity of the molecular chains at high temperatures relaxed the recrystallization-induced stress to some extent. Therefore, no cracks were observed until 80 h had passed. However, in PP-S-I, the synergistic effect of these negative changes finally destroyed the film.

### CONCLUSIONS

As opposed to the widely accepted thermal oxidation mechanism, the deterioration of the PP/SiO<sub>2</sub> nanocomposite under a thermal oxidation atmosphere was found not to be caused by oxidative degradation, nor was there a consequent decrease in the weight-average molecular weight. At 130°C, the recrystallization happened. Both the spherulite size and crystallinity increased significantly, whereas the amorphous region almost disappeared. During the recrystallization, the nanoparticles, as impurities, were rejected to the spherulite boundaries, which made them weak. If the sample suffered from violent temperature changes, a large difference in the expansion coefficient between the matrix and the nanoparticles tore the particles from the matrix and left voids in the interface or cracks along the spherulite boundaries. All of these aspects were responsible for the rapid damage of the PP/SiO<sub>2</sub> film and that is why the PP and PP-S-C remained stable. In sum-

mary, physical changes may overwhelm chemical changes and dominate the property deterioration of polymer materials, especially composites, under certain conditions.

### References

1. Ray, S. S.; Okamoto, M. *Prog Polym Sci* 2003, 28, 1539.
2. Ellis, T. S.; D'Angelo, J. S. *J Appl Polym Sci* 2003, 90, 1639.
3. Maiti, P.; Nam, P. H.; Okamoto, M.; Kotaka, T.; Hasegawa, N.; Usuki, A. *Macromolecules* 2002, 35, 2042.
4. Maiti, P.; Nam, P. H.; Okamoto, M.; Kotaka, T.; Hasegawa, N.; Usuki, A. *Polym Eng Sci* 2002, 42, 1864.
5. Mishra, S.; Sonawane, S. H.; Singh, R. P. *J Polym Sci Part B: Polym Phys* 2005, 43, 107.
6. Lloyd, S. M.; Lave, L. B. *Environ Sci Technol* 2003, 37, 3458.
7. Blumstein, A. *J Polym Sci Part A: Gen Pap* 1965, 3, 2665.
8. Gilman, J. W.; Jackson, C. L.; Morgan, A. B.; Harris, P.; Manias, E.; Giannelis, E. P.; Wuthenow, M.; Hilton, D.; Phillips, S. H. *Chem Mater* 2000, 12, 1866.
9. Morgan, A. B.; Harris, R. H.; Kashiwagi, T.; Chyall, L. J.; Gilman, J. W. *Fire Mater* 2002, 26, 247.
10. Bertini, F.; Canetti, M.; Audisio, G.; Costa, G.; Falqui, L. *Polym Degrad Stab* 2006, 91, 600.
11. Zanetti, M.; Camino, G.; Reichert, P.; Mulhaupt, R. *Macromol Rapid Commun* 2001, 22, 176.
12. Zanetti, M.; Bracco, P.; Costa, L. *Polym Degrad Stab* 2004, 85, 657.
13. Qin, H. L.; Zhang, S. M.; Zhao, C. G.; Feng, M.; Yang, M. S.; Shu, Z. J.; Yang, S. S. *Polym Degrad Stab* 2004, 85, 807.
14. Lomakin, S. M.; Dubnikova, I. L.; Berezina, S. M.; Zaikov, G. E. *Polym Int* 2005, 54, 999.
15. Zhu, J.; Uhl, F. M.; Morgan, A. B.; Wilkie, C. A. *Chem Mater* 2001, 13, 4649.
16. Xu, Y.; Brittain, W. J.; Xue, C.; Eby, R. K. *Polymer* 2004, 45, 3735.
17. Chen, K.; Vyazovkin, S. *Macromol Chem Phys* 2006, 207, 587.
18. Chatterjee, A.; Deopura, B. L. *J Appl Polym Sci* 2006, 100, 3574.
19. Peprnicek, T.; Simonik, J.; Achillesova, J.; Kuritka, I.; Saha, P.; Plestil, J.; Pavlova, E. *Int J Polym Anal Charact* 2006, 11, 455.
20. Filho, F. G. R.; Melo, T. J. A.; Rabello, M. S.; Silva, S. M. L. *Polym Degrad Stab* 2005, 89, 383.
21. Knight, J. B.; Calvert, P. D.; Billingham, N. C. *Polymer* 1985, 26, 1713.
22. Fayolle, B.; Audouin, L.; Verdu, J. *Polym Degrad Stab* 2000, 70, 333.
23. Fayolle, B.; Audouin, L.; Verdu, J. *Polym Degrad Stab* 2002, 75, 123.
24. Fayolle, B.; Audouin, L.; Verdu, J. *Polymer* 2004, 45, 4323.
25. Li, J. F.; Yang, R.; Yu, J.; Liu, Y. *Polym Degrad Stab* 2008, 93, 84.
26. Calvert, P. D.; Ryan, T. G. *Polymer* 1978, 19, 611.
27. Li, J. F.; Yang, R.; Yu, J.; Liu, Y. *Polym Eng Sci* 2008, 24, 103.